American Journal of Pathology, Vol. 146, No. 4, April 1995

Establishment and Characterization of Two Divergent Cell Lines Derived from a Human Chromophobe Renal Cell Carcinoma

Claus Dieter Gerharz,* Roland Moll,† Stefan Störkel,† Uwe Ramp,* Barbara Hildebrandt,‡ Gabriele Molsberger,§ Pavel Koldovsky,‖ and Helmut Erich Gabbert*

From the Institutes of Pathology and Human Genetics and Anthropology‡ and the Departments of Gastroenterology§ and Otorhinolaryngology,‖ University Hospital of Düsseldorf, Düsseldorf, and the Institute of Pathology,† University Hospital of Mainz, Mainz, Germany*

The chromophobe renal cell carcinoma is a distinct type of renal cancer presumably derived from the intercalated cell of the collecting duct system and exhibiting a better prognosis than other types of renal cell carcinoma. Chromophobe carcinomas can be separated from other types of renal cell carcinoma by their characteristic cytomorphology, ultrastructural appearance, cytoskeletal architecture, and cytogenetic aberrations. As no permanent cell line of the chromophobe tumor type has previously been described, we are the first to report on the successful establishment and characterization of two divergent permanent cell lines, ie, chrompho-A and chrompho-B, derived from the same chromophobe renal cell carcinoma. With immunocytochemistry, two-dimensional gel electrophoresis, and Western blot, chrompho-A and chrompho-B exclusively exhibited cytokeratins (Nos. 7, 8, 18, and 19) but not vimentin. Ultrastructural studies revealed numerous cytoplasmic microvesicles as well as coated vesicles that are known to be characteristic features of the intercalated cell. Chrompho-B cells exhibited a shorter mean population doubling time (t_D = 43 hours) than chrompho-A cells (t_D = 51 hours). Both cell lines failed to produce tumors in nude mice with the subrenal capsule assay. Cytogenetic analyses revealed hyperdiploid chromosome numbers in both cell lines with telomeric associations as well as numeric aberrations known from chromophobe renal cell carcinomas in vivo. (Am J Pathol 1995, 146:953–962)

The chromophobe carcinoma is a distinct type of renal cancer first described in humans by Thoenes et al.[1] The chromophobe carcinoma resembles the clear cell carcinoma, likewise showing tumor cells with a highly transparent cytoplasm. In contrast to the clear cell type of renal carcinoma, however, chromophobe tumor cells exhibit a fine reticular (not empty) cytoplasm. The cytomorphological separation between clear and chromophobe renal cell carcinomas was further substantiated by differences of ultrastructural appearance, cytoskeletal architecture, enzyme synthesis, and cytogenetic aberrations.[2–10] Furthermore, convincing arguments have been accumulated in the meantime suggesting that the clear cell carcinoma originates from the proximal tubular system whereas the chromophobe tumor cells closely resemble the intercalated cells of the cortical collecting duct system.[5,11–14] The difference in histogenetic derivation of chromophobe and clear renal cell carcinomas is also reflected by differences in the biological behavior of these tumor types, with the clear cell carcinoma exhibiting a worse prognosis.[15] Although quite a number of renal carcinoma cell lines have been established during recent years,[16–19] no cell line derived from a chromophobe renal cell carcinoma has been established so far. Therefore, we are the first to report on the establishment and characterization of two divergent cell lines derived from a human chromophobe renal cell carcinoma.

Supported by the Deutsche Forschungsgemeinschaft.

Accepted for publication December 8, 1994.

Dedicated to Prof. Dr. Wolfgang Thoenes (died in 1992).

Address reprint requests to Dr. C. D. Gerharz, Institute of Pathology, Heinrich-Heine-University, Moorenstr. 5, D-40001 Düsseldorf, Germany.

Materials and Methods

Cell Culture

During the last 4 years, 14 different chromophobe renal cell carcinomas have been available for cultivation *in vitro*. Tumor samples were obtained immediately after nephrectomy and minced under aseptic conditions with paired scissors. The resulting mechanically macerated tissue mass was repeatedly washed by centrifugation and finally seeded into 25-cm^2 Nunclon culture flasks (GIBCO, Karlsruhe, Germany) with Dulbecco's modified Eagle's medium (GIBCO) supplemented with 10% fetal calf serum, penicillin, and streptomycin. The cultures were maintained at 37 C in an atmosphere with 5% CO_2. For subculturing, cells were disaggregated by exposure to 0.05% EDTA (Biochrom, Berlin, Germany). Of 14 chromophobe renal cell carcinomas 13 could be established only as short-term cultures for passage numbers ranging from 2 to 18 and different time periods ranging from 4 weeks to 8 months. Only 1 of the 14 different chromophobe renal cell carcinomas gave rise to two divergent permanent cell lines, named chrompho-A and chrompho-B. These cell lines were derived from the chromophobe carcinoma of an 83-year-old female patient (tumor stage according to the Union Internationale Contre le Cancer, pT3a pNX pMX). The two cell lines are presently at the 54th (chrompho-A) and 67th (chrompho-B) passage after 24 months in permanent culture. Most of our studies were performed with cells from passages 20 to 30, describing the two cell lines at an early *in vitro* stage. Nevertheless, the cytomorphological features of these cell lines proved to be remarkably stable up to the present passages.

Light Microscopy

Tumor tissue of the original tumor was fixed in 4% formaldehyde and embedded in paraplast. The tumor cells cultivated *in vitro* were seeded on microscope slides and fixed *in situ* by immersion into 4% formaldehyde. The slides were stained with hematoxylin and eosin (H&E) and periodic acid schiff hemalum. Lipid staining with Sudan IV was performed on cryostat sections of the formalin-fixed original tumor.

Immunohistochemistry

Formalin-fixed, paraffin-embedded tissue samples of the original tumor had to be used for immunohistochemistry of intermediate filaments. After microwave oven pretreatment of the deparaffinized sections and mild trypsinization (0.001% trypsin), the paraffin sections were stained for simple epithelial cytokeratins and vimentin (for primary antibodies, see Table 1) by the avidin-biotin complex peroxidase method (for details see Ref. 20). The cultivated tumor cells were seeded on microscope slides, fixed *in situ* by exposure to methanol (5 minutes) and acetone (10 seconds) at −20 C, and then air dried and stored at −20 C. Before staining, an additional acetone fixation (5 minutes at −20 C) was performed followed by air drying. Primary antibodies (Table 1) were applied to the slides and allowed to incubate for 30 minutes at room temperature in a moist chamber. The visualization of the primary antibodies was achieved by the indirect immunoperoxidase method.[4]

Gel Electrophoresis and Western Blotting

Cytoskeletal residues of the cell lines, obtained by extraction with a high salt detergent buffer and a low salt buffer[21] were analyzed by two-dimensional gel electrophoresis with nonequilibrium pH gradient electrophoresis in the first dimension, and sodium dodecyl sulfate polyacrylamide gel electrophoresis in the second dimension. Gels were stained by either

Table 1. *List of Antibodies Used*

	Antibody	Specificity	Source
Paraffin sections of the original tumor			
	Mab K_s 7.18	Cytokeratin 7	Progen Biotechnics, Heidelberg, Germany
	Mab CAM 5.2	Cytokeratin 8	Becton Dickinson, Neckargemünd, Germany
	Mab K_s 19.1	Cytokeratin 19	Progen Biotechnics
	Mab IT-K_s 20.8, IT-K_s 20.6	Cytokeratin 20	Progen Biotechnics
	Mab VIM-3B4	Vimentin	Progen Biotechnics
Cell cultures and Western blotting			
	Mab CK-7	Cytokeratin 7	Boehringer, Mannheim, Germany
	Mab K_s 18.174	Cytokeratin 18	Progen Biotechnics
	Mab K_s 19.2.Z105	Cytokeratin 19	Progen Biotechnics
	Mab IT-K_s 20.5	Cytokeratin 20	Progen Biotechnics
	Mab VIM-9	Vimentin	Viramed, Martinsried, Germany

Mab, mouse monoclonal antibody.

Coomassie brilliant blue or a highly sensitive silver staining method.[21] Western blotting was performed according to standard procedures (for details see Ref. 21). For primary antibodies see Table 1). Bound antibodies were detected by using peroxidase-conjugated rabbit antibodies against mouse immunoglobulins (Dako Corp., Carpenterio, CA). The staining reaction was performed by using 3,3′-diaminobenzidine, H_2O_2, and $NiSO_4$.

Scanning Electron Microscopy

For scanning electron microscopy, tumor cells seeded on glass cover slips were fixed by exposure to 2.5% phosphate-buffered glutaraldehyde solution (pH 7.2) and postfixed in 2% osmium tetroxide solution. After dehydration in an ascending acetone series, the tumor cell monolayer was dried by the critical point method and sputtered with gold. Electron photomicrographs were taken with a PSEM 510 scanning electron microscope.

Transmission Electron Microscopy

For transmission electron microscopy, tumor cells seeded on glass cover slips were fixed *in situ* by exposure to 2.5% sodium cacodylate-buffered glutaraldehyde solution (0.1 mol/L, pH 7.4) and postfixed in 1% sodium cacodylate-buffered osmium tetroxide solution (0.1 mol/L, pH 7.4) before Epon embedding *in situ*. Thin sections were contrasted with uranyl acetate and lead citrate. Electron photomicrographs were taken with an EM 410 Philips transmission electron microscope.

Growth Properties In Vitro

Doubling Time

Altogether, 24 replicate 25-cm^2 culture flasks received inocula of 2×10^5 cells each. Cells from 4 culture flasks were harvested separately on days 3, 4, 5, 7, 9, and 11 after inoculation. Cell counts were performed with the Neubauer hemocytometer. The results were plotted on semi-logarithmic paper and the mean population doubling time was determined during the exponential growth phase.

Saturation Density

The maximal number of tumor cells present in 25-cm^2 culture flasks was determined during the plateau phase of growth.

Plating Efficiency

Tumor cells were seeded into 96-microwell plates (GIBCO) at definite concentrations (ranging from 1 to 100 cells per microwell) and incubated in a humidified atmosphere of 5% CO_2 for 4 weeks. The plating efficiency was determined as the number of microwells with visible colonies relative to the number of microwells inoculated with tumor cells.

Tumorigenicity in Nude Mice

For tumorigenicity testing, tumor cells were implanted under the renal capsule of four nude mice per cell line, according to a procedure previously described by Fingert et al.[23] Briefly, 8×10^6 tumor cells were washed in phosphate-buffered saline by repeated centrifugation. The cell pellet obtained was suspended in 10 µl of phosphate-buffered saline supplemented with fibrinogen (20 mg/ml). After careful resuspension, 5 µl of thrombin dissolved in minimal essential medium (20 U/ml) were added. The clot forming after incubation at 37 C for 10 minutes was cut in four pieces, and each piece was inserted under the renal capsule of a 6-week-old female nude mouse. After 4 months, the animals were sacrificed and histological examination of kidneys and lungs was performed.

Flow Cytometric DNA Measurement

Exponentially growing tumor cells of passages 14 and 40 were harvested and resuspended in dimethylsulfoxide citrate buffer for storage in liquid nitrogen.[24] For DNA analysis, the tumor cells were thawed and further processed according to a method described by Vindelov et al.[25] Briefly, the tumor cells were treated with trypsin (20 µg/ml) for 10 minutes and RNAse A (40 µg/ml) for 10 min. The cell nuclei obtained were stained with propidium iodide (120 µg/ml), and 1.5×10^4 nuclei were analyzed by using a flow cytophotometer (FACScan, Becton Dickinson, Heidelberg, Germany). Chicken red blood cells were used in additional measurements as an internal calibration standard for DNA ploidy, the DNA contents of chicken red blood cells being 38% of the human diploid value.[25] The ploidy level of the tumor cells was expressed as DNA index, the DNA index of diploid human cells being 1.0.

Chromosome Analysis

Chromosome preparations were obtained by using standard hypotonic pretreatment procedures at early

passages (20 to 22). G-banding was performed by applying the technique of Seabright.[26] A total of 30 G-banded metaphases per cell line were analyzed, and 11 metaphases were karyotyped from each cell line. Description of karyotypes was done according to the International System for Human Cytogenetics Nomenclature.[27]

Results

Original Tumor

The original tumor was a typical representative of the chromophobe type of renal cell carcinoma as previously described.[1,2] In H&E-stained sections, the voluminous tumor cells showed a translucent but finely reticular cytoplasma (Figure 1a). The cell boundaries were markedly pronounced so that the tumor cells were clearly demarcated from one another. Periodic acid Schiff and lipid staining revealed no appreciable amounts of glycogen and lipid. In contrast, the Hale staining for acid mucopolysaccharides showed an intense diffuse reaction of the cytoplasm. The nuclei were moderately enlarged corresponding to a G2 grade of malignancy. Immunohistochemically, no expression of vimentin (Figure 1b) could be demonstrated, whereas a positive staining reaction with antibodies against cytokeratins 7 (Figure 1c) and 8 (Figure 1d) was observed. Cytokeratin 7 was restricted to scattered tumor cell groups, preferentially facing the stroma or accumulations of debris, whereas cytokeratin 8 was present in all tumor cells. Cytokeratin 19 could be detected immunohistochemically in tiny groups of tumor cells, the distribution pattern corresponding to that of cytokeratin 7 (not shown). Cytokeratin 20 was not observed in the tumor cells.

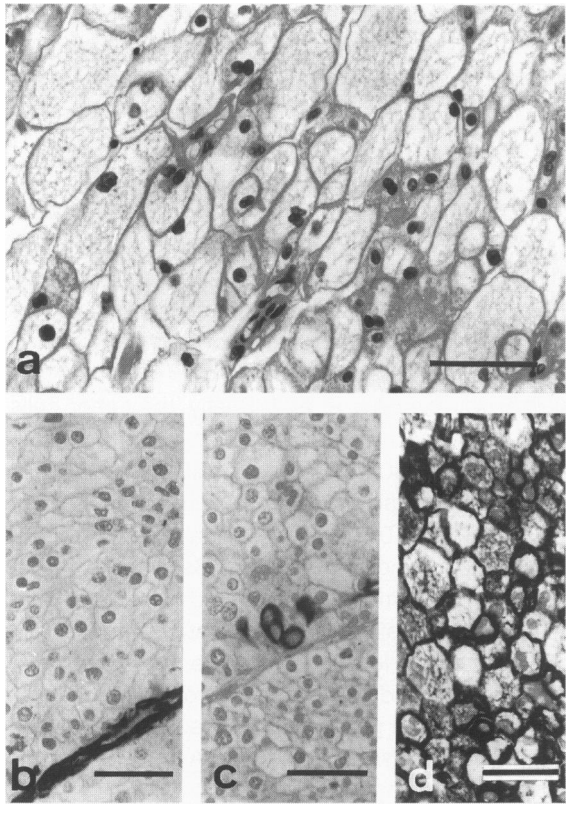

Figure 1. *Cytomorphological and immunohistochemical aspects of the original chromophobe renal cell carcinoma. Voluminous tumor cells show a translucent but finely reticular cytoplasm and prominent cell boundaries* (a). *There was no staining reaction of the tumor cells for vimentin* (b) *and a positive staining reaction of some tumor cells for cytokeratin 7* (c) *and of most tumor cells for cytokeratin 8* (d). *Bars = 50 μ.*

Cell Lines

Two divergent cell lines, ie, chrompho-A and chrompho-B, could be derived from the same original tumor. As shown by scanning electron microscopy (Figure 2a, f), both cell lines grow strictly anchorage dependent as monolayers. Periodic acid Schiff staining revealed no appreciable deposits of glycogen and Hale staining for acid mucopolysaccharides produced a diffuse but sometimes also finely granular staining of the cytoplasma (not shown).

Immunocytochemically, the tumor cells of chrompho-A and chrompho-B did not show a staining reaction with antibodies against vimentin (Figure 2b, g). Antibodies against cytokeratins 7 (Figure 2c, h), 18 (Figure 2d, i), and 19 (Figure 2e, j) produced a positive staining reaction in both cell lines with marked differences in the proportion of reacting cells (Table 2).

Two-dimensional gel electrophoresis (Figure 3a, b) revealed that the primary simple epithelial cytokeratins 8 and 18 were clearly predominant in both cell lines. In addition, small but significant amounts of cytokeratin 7 were apparent in the gels as small protein spots. A specific positive reaction in Western blotting (Figure 3c, d) with the cytokeratin 7 antibody proved that the minor spots in fact represented cytokeratin 7. Only very faint cytokeratin 19 spots were noted in the gels, which are not visible in the photographic reproductions. No reaction was obtained in Western blotting experiments with the vimentin antibody (not shown).

By transmission electron microscopy, no major differences became evident between both cell lines. The tumor cells of both cell lines were loosely apposed, showing extended cytoplasmatic protrusions (Figure 4a). A prominent ultrastructural feature of both

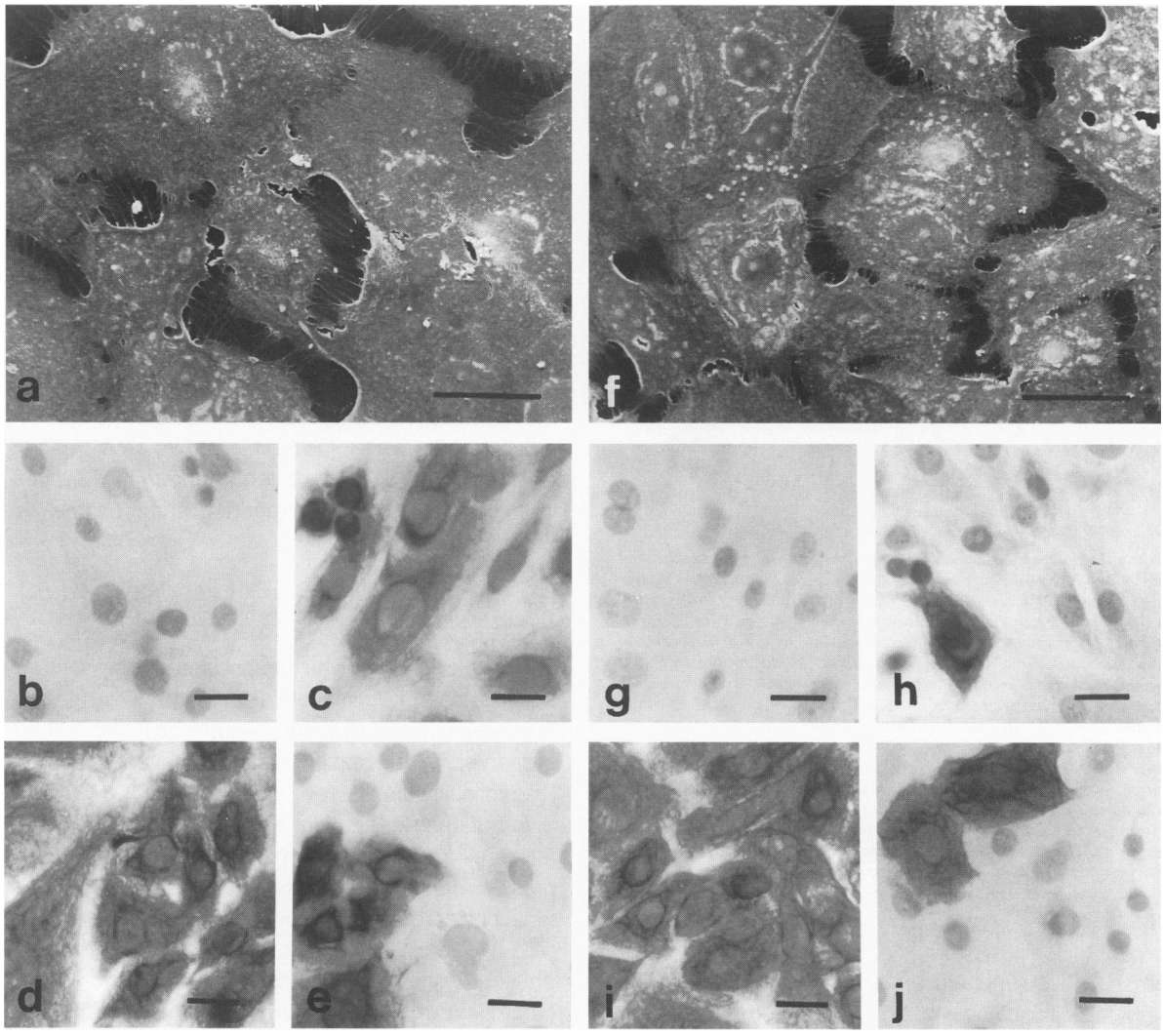

Figure 2. *Cytomorphological and immunohistochemical aspects of chrompho-A* (**a** *to* **e**) *and chrompho-B* (**f** *to* **j**). *Scanning electron microscopic aspect of chrompho-A* (**a**) *and chrompho-B* (**f**) *showing loosely apposed tumor cells with abundant cytoplasmic microspikes. There was no staining reaction for vimentin in chrompho-A* (**b**) *and chrompho-B* (**g**) *and a positive staining reaction for cytokeratins 7* (**c** *and* **h**), *18* (**d** *and* **i**), *and 19* (**e** *and* **j**) *in chrompho-A* (**c**, **d**, *and* **e**) *and chrompho-B* (**h**, **i**, *and* **j**). *Bars = 25 μ.*

Table 2. *Percentage of Positive Tumor Cells for Vimentin and Cytokeratin Polypeptides*

		Cytokeratin			
	Vimentin	7	18	19	20
Chrompho-A	0%	50%	100%	40%	0%
Chrompho-B	0%	10%	100%	10%	0%

chrompho-A and chrompho-B cells were cytoplasmic microvesicles (diameter, 100 to 300 nm) that were predominantly located near the apical surface as revealed by tangential (Figure 4b) and vertical (Figure 4c) sections. The microvesicles near the apical surface were often continuous with the extracellular space, whereas microvesicles deeper in the cytoplasm proved to be closed structures. Furthermore, both chrompho-A and chrompho-B cells exhibited coated vesicles located deep in the cytoplasm (Figure 4d) as well as near the cell surface (Figure 4e), suggesting a process of membrane fusion or endocytosis. Another type of microvesicle frequently observed in chrompho-A and chrompho-B cells is characterized by the concentric grouping of small vesicles around a central vesicle (Figure 4f), the latter sometimes being continuous with the extracellular space.

The *in vitro* growth properties of chrompho-A and chrompho-B cells are shown in Figure 5. Chrompho-B cells exhibited a shorter mean population doubling time (t_D = 43 hours) and a higher saturation density ($4.1 \times 10^4 \pm 0.4 \times 10^4$ cells/cm^2) than chrompho-A cells (t_D = 51 hours and $2.8 \times 10^4 \pm 0.4 \times 10^4$ cells/

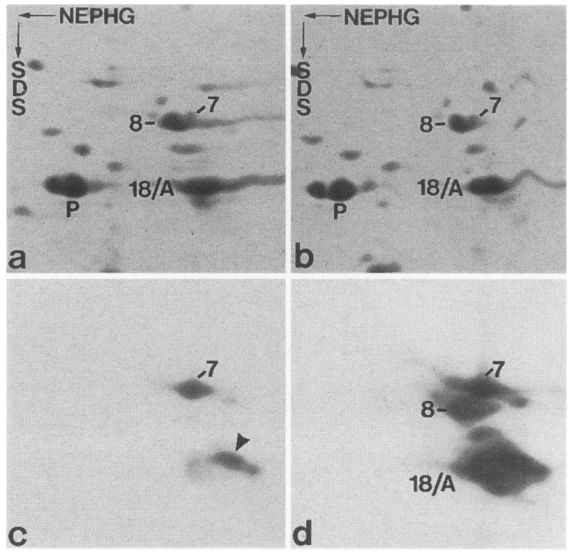

Figure 3. *Biochemical analysis of cytokeratin polypeptides in chrompho-A* (a) *and chrompho-B* (b *to* d). *Two-dimensional gel electrophoresis (Coomassie blue staining) of cytoskeletal preparations obtained from chrompho-A* (a) *and chrompho-B* (b) *cells by nonequilibrium plt gradient (NEPHG) electrophoresis in the first dimension and sodium dodecyl sulfate polyacrylamide gel electrophoresis (SDS) in the second dimension. Cytokeratin polypeptides are denoted by numbers. Note the presence of small but significant amounts of cytokeratin 7 in both cell lines, next to the main cytokeratins 8 and 18. Western blot* (c) *derived from a two-dimensional gel corresponding to that shown in* (b), *with antibody CK-7 against cytokeratin 7 compared with the subsequent India ink staining of the same nitrocellulose membrane* (d) *provides proof that the spot designated CK-7 truly represents this particular cytokeratin polypeptide. In addition, the antibody CK-7 also recognizes a degradation product derived therefrom (arrowhead in* c). *P, 3-phosphoglycerokinase from yeast, added as marker protein; A, endogenous actin.*

cm^2). The plating efficiency of both cell lines was rather low, requiring a minimum inoculum of 100 cells per microwell (Table 3).

Unfortunately, both cell lines failed to produce tumors in nude mice after an observation period of up to 4 months by the subrenal capsule assay. The cytophotometrically determined DNA distribution revealed DNA aneuploidy in both cell lines (Figure 6). Each cell line exhibited two DNA stem lines, the DNA index being 1.35 and 2.7 for chrompho-A tumor cells and 1.3 and 2.6 for chrompho-B tumor cells. As suggested by the ratio between the DNA indices, the coexistence of two DNA stem lines in each cell line is probably explained by a process of endomitosis. The DNA indices proved to be stable when tumor cells of passages 14 and 40 were analyzed. Due to the coexistence of two DNA stem lines, cell cycle analysis could not be performed.

Cytogenetic analyses revealed hyperdiploid chromosome numbers in chrompho-A and chrompho-B (Table 4 and Figure 7). Both cell lines showed chromosomal diploidy for the chromosomes 1, 2, 6, 13, 17, 18, 21, and 22. Numerical chromosomal aberrations involving both cell lines were observed for the chromosomes 4, 5, 7, 8, 9, 11, 12, 15, 16, and 19 resulting in either trisomy or tetrasomy. Structural chromosomal abnormalities were seen in both cell lines on the short arm of two extra chromosomes 8 as well as in the form of two extra derivative chromosomes 12. Furthermore, telomeric associations (Fig. 7c) were observed in 9 of 30 chrompho-A and in 5 of 30 chrompho-B metaphases analyzed. Chrompho-B consistently showed additional structural abnormalities that permitted a clear cytogenetic separation from chrompho-A, ie, a terminal deletion of 1q, a triploidy of 3p in combination with a loss of 3q, and in three metaphases a translocation of the long arms of chromosomes 7 and 13. Furthermore, two small marker chromosomes were observed in chrompho-B differing from the single marker chromosome in chrompho-A.

Discussion

The results of our investigation clearly demonstrate that the essential cytoskeletal, ultrastructural, and cytogenetic features of the chromophobe tumor cell are preserved in permanent cell lines even after prolonged cultivation.

In contrast to the clear and chromophilic types of renal cell carcinoma, which nearly consistently coexpress vimentin and cytokeratins, the chromophobe renal cell carcinoma exhibits exclusively cytokeratins (7, 8, 18, and 19) but not vimentin.[3,4,6,28] We have previously shown that cell lines derived from clear cell carcinomas maintain the typical intermediate filament phenotype of the original tumors, ie the coexpression of simple epithelial cytokeratins and vimentin.[29,30] Here we present evidence that an analogous conservatism holds true for permanent cell lines derived from chromophobe carcinoma. In fact, the complete absence of vimentin in chrompho-A and chrompho-B is a noteworthy finding, as a coexpression of vimentin together with cytokeratins is a feature of many epithelial cell lines derived from various types of carcinomas showing no vimentin expression in the original tumor.[31] Concerning the individual cytokeratin polypeptides, chromophobe carcinomas frequently exhibit a quantitative predominance of cytokeratin 7 over cytokeratin 19, much in contrast to clear cell and chromophilic renal carcinomas.[3,4] This observation was also apparent in the present cell lines, particularly in gel electrophoresis. Therefore, the intermediate filament profile of chrompho-A and chrompho-B further underlines the high conservatism of the chromophobe cell phenotype after prolonged *in vitro* culture.

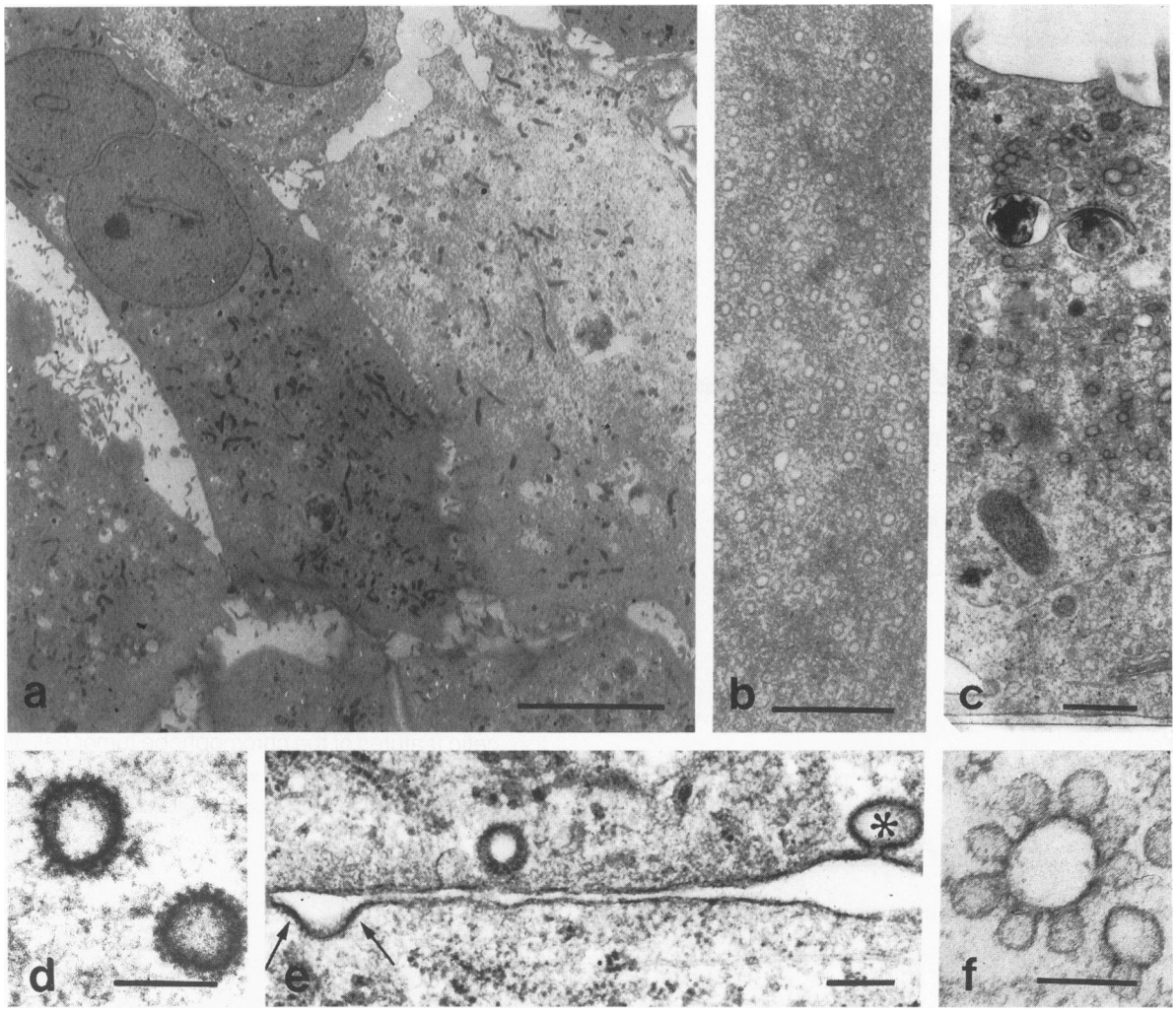

Figure 4. *Ultrastructural aspects of chrompho-A and chrompho-B. Loosely apposed tumor cells show cytoplasmic microspikes* (a) *and abundant cytoplasmic microvesicles* (b *and* c) *concentrated near the apical surface as revealed by tangential* (b) *and vertical* (c) *sectioning. Coated vesicles are seen deep in the cytoplasma* (d) *and near the cell surface* (e). *Note the close relation of coated vesicles to the plasmalemma* (e, *) *and the circumscribed thickening of the plasmalemma* (e, *arrows*), *suggesting a process of membrane fusion or endocytosis. Concentric grouping of microvesicles around a central vesicle* (f) *is shown.* a, *bar = 20 μ;* b *to* f, *bars = 0.5 μ.*

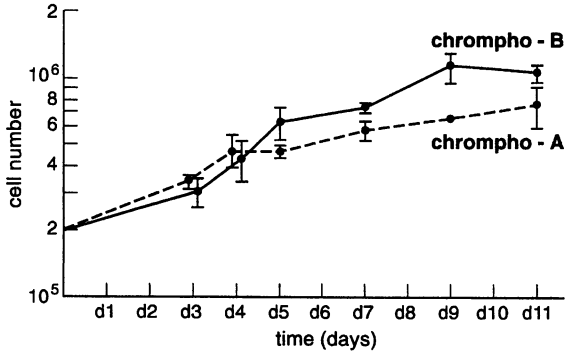

Figure 5. *Growth curves of chrompho-A and chrompho-B. Each value represents the mean ± standard deviation of four experiments.*

Table 3. *Plating Efficiency of Chrompho-A and Chrompho-B*

Number of cells seeded per microwell	Plating efficiency after 14 days	28 days
Chrompho-A		
1	0%	0%
10	0%	0%
100	3%	6%
Chrompho-B		
1	0%	0%
10	0%	0%
100	7%	8%

Microvesicles are a characteristic ultrastructural feature of the chromophobe tumor cell *in vivo*[1,2,4] and are also known from the intercalated cell, which has been observed in the collecting duct system of rat and human kidneys.[5,32–36] Therefore, it has been proposed that the chromophobe carcinoma might originate from the intercalated cell.[5] The close resemblance between chromophobe tumor cells and the

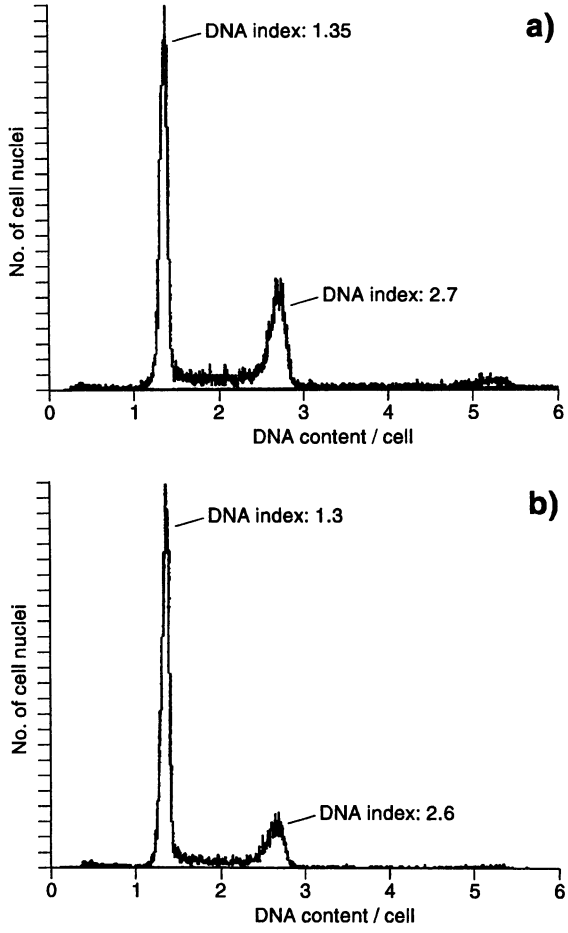

Figure 6. *Flow cytometric DNA histogram of chrompho-A* (a) *and chrompho-B* (b).

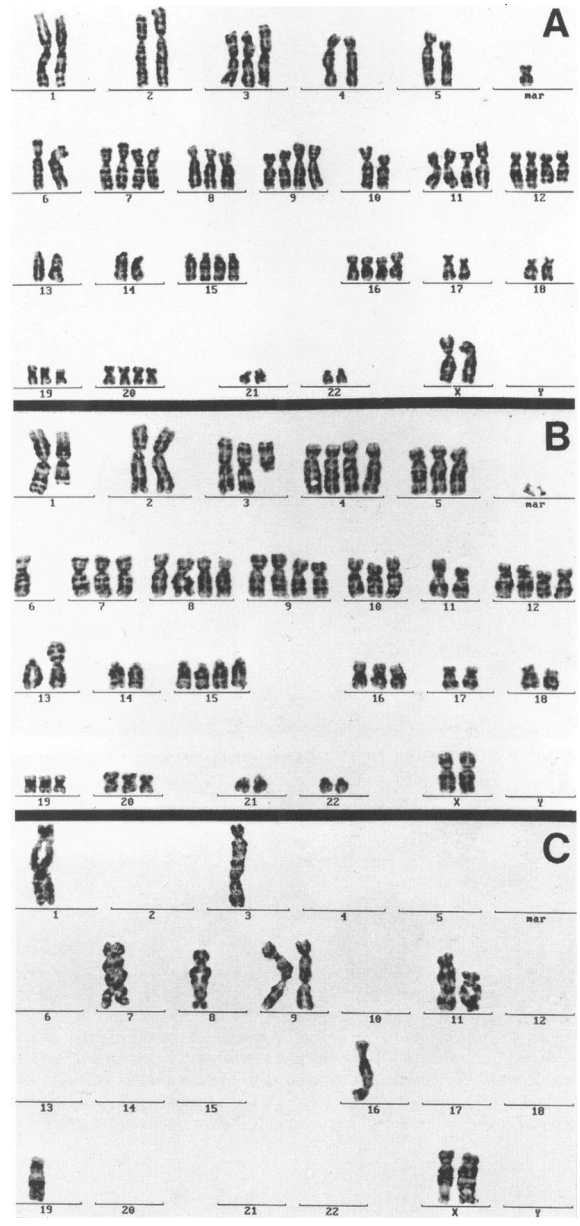

Figure 7. *Chromosome analysis. Representative karyotype of a chrompho-A* (A) *and chrompho-B* (B) *tumor cell and examples of telomeric associations* (C) *observed in chrompho-A and chrompho-B are shown.*

intercalated cell of the collecting duct system was further confirmed by our *in vitro* observations, demonstrating abundant cytoplasmic microvesicles in both chrompho-A and chrompho-B cells. Most importantly, however, both cell lines exhibited clathrin-like coated vesicles located deep in the cytoplasm as well as near the cell surface. These coated vesicles had not previously been observed in chromophobe renal cell carcinomas *in vivo*.[5] As coated vesicles are a characteristic feature of the intercalated cell type,[5,33,36] the observation of this type of vesicle in our cell lines further supports the relation between the chromophobe tumor cell and the intercalated cell. Coated vesicles are supposed to contain a major protein component of the ATP-driven proton pump H^+-ATPase[37] and have been shown to fuse with the luminal plasmalemma of intercalated cells.[32,33] On the other hand, the retrieval of water channels from the

Table 4. *Description of Karyotypes in Accordance with ISCN (1991)*

Cell line	Description of karyotype
Chrompho-A	58–65,XX,+3,+4,+5,+7,+7,+2xder(8)t(8;?)(q;?),+9,+9,+11,+11,+2xder(12)(12 pter→q13::10q23→qter),+15,+15,+16,+16,+19,+20,+20,+mar
Chrompho-B	55–64,XX,der(1)del(1)(q32),+3p,+4,+4,+5,+7,+2xder(8)t(8;?)(q;?),+9,+9,+10,+11,+11,+2xder(12)(12pter→q13::10q23→qter),+t(7;13)(q;q),+14,+15,+15,+16,+19,+mar,+mar

apical membrane of intercalated cells has been suggested to be associated with endocytosis via coated pits.[38] Therefore, it was interesting to observe coated vesicles in close relation to the plasmalemma of chrompho-A and chrompho-B cells, suggesting a preserved process of membrane fusion or endocytosis.

Only a few cytogenetic analyses of chromophobe carcinomas have been reported so far.[8–10] From these publications, telomeric associations, the gain of chromosomes (3, 5, 7, 8, 12, 16, 18, 19, and 20) as well as the loss of chromosomes (1, 2, 6, 10, 11, 13, 14, 17, 18, and 21) seem to be the most important characteristics of chromophobe carcinomas. Corresponding structural and numerical chromosomal abnormalities also became evident for our cell lines chrompho-A and chrompho-B, showing telomeric association and a marked gain of chromosomes, especially the gain of chromosomes 5, 7, 8, 12, 16, and 19, which was observed in both cell lines, and had previously been published for chromophobe carcinomas.[8–10] The marked congruence of numerical and structural chromosomal abnormalities observed between chrompho-A and chrompho-B underlined the derivation from the same original tumor. Nevertheless, chrompho-A and chrompho-B can be considered as two cytogenetically distinct cell lines, as became evident from structural abnormalities present in chrompho-B cells but missing in chrompho-A cells.

In conclusion, the results of our investigation demonstrate that characteristic morphological and cytogenetic features of the chromophobe tumor cell are preserved in the cell lines chrompho-A and chrompho-B. Therefore, these cell lines will become valuable tools for additional investigations into the genetic, molecular, and biological properties of the chromophobe type of renal cell carcinoma. Experimental studies analyzing the effects of biological response modifiers on the proliferation and invasive behavior of these cell lines are currently in progress in our laboratory. Additional studies will also have to show whether the functional properties of the intercalated cell type have been preserved in our cell lines to the same extent that was observed for structural characteristics. In that case, our cell lines might also become an appropriate *in vitro* model for investigations into the physiology of the intercalated cell type.

Acknowledgments

We express our appreciation to Mrs. U. Herian, Mrs. A. Florange, Mrs. H. Balven, Mrs. U. Ludolf, Mrs. M. Müller, Mrs. R. Baumann, Mrs. A. Holzbach, Mr. P. Pulkowski, Mr. M. Ringler, Mr. F. Rinschede, and Mrs. H. Auweiler for their excellent technical assistance.

References

1. Thoenes W, Störkel ST, Rumpelt HJ: Human chromophobe cell renal carcinoma. Virchows Arch B Cell Pathol 1985, 48:207–217
2. Thoenes W, Störkel ST, Rumpelt HJ: Histopathology and classification of renal cell tumors (adenomas, oncocytomas, and carcinomas). Pathol Res Pract 1986, 181:125–143
3. Pitz S, Moll R, Störkel S, Thoenes W: Expression of intermediate filament proteins in subtypes of renal cell carcinomas and in renal oncocytomas. Lab Invest 1987, 6:642–653
4. Thoenes W, Störkel S, Rumpelt HJ, Moll R, Baum HP, Werner S: Chromophobe cell renal carcinoma and its variants: a report on 32 cases. J Pathol 1988, 155: 277–287
5. Störkel S, Steart PV, Drenckhahn D, Thoenes W: The human chromophobe cell renal carcinoma: its probable relation to intercalated cells of the collecting duct. Virchows Arch B Cell Pathol 1989, 56:237–245
6. Bonsib SM, Lager DJ: Chromophobe cell carcinoma: analysis of five cases. Am J Surg Pathol 1990, 14: 260–267
7. Erlandson RA, Reuter VE: The quarterly case: renal tumor in a 62-year-old male. Ultrastruct Pathol 1988, 12: 561–567
8. Crotty TB, Lawrence KM, Moertel CA, Bartelt DH, Batts KP, Dewald GW, Farrow GM, Jenkins RB: Cytogenetic analysis of 6 renal oncocytomas and a chromophobe cell renal carcinoma: evidence that -Y, -1 may be a characteristic anomaly in renal oncocytomas. Cancer Genet Cytogenet 1992, 61:61–66
9. Van den Berg E, van der Hout AH, Oosterhuis JW, Störkel S, Dijkhuizen T, Dam A, Zweers HMM, Mensink HJA, Buys CHCM, de Jong B: Cytogenetic analysis of epithelial renal cell tumors: relationship with a new histopathological classification. Int J Cancer 1993, 55: 223–227
10. Kovacs G: Molecular differential pathology of renal cell tumors. Histopathology 1993, 22:1–8
11. Bachmann S, Kriz W, Kuhn C, Franke WW: Differentiation of cell types in the mammalian kidney by immunofluorescence microscopy using antibodies to intermediate filament proteins and desmoplakins. Histochemistry 1983, 77:365–394
12. Holthöfer H, Miettinen A, Paasivou R, Lehto V-P, Linder E, Alfthan O, Virtanen I: Cellular origin and differentiation of renal cell carcinomas: a fluorescence microscopic study with kidney-specific antibodies, antiintermediate filament antibodies and lectins. Lab Invest 1983, 49:317–326
13. Waldherr R, Schwechheimer K: Co-expression of cytokeratin and vimentin intermediate-sized filaments in

renal cell carcinomas. Virch Arch A Pathol Anat Histol 1985, 408:15–27
14. Oosterwijk E, Van Muijen GNP, Oosterwijk-Wakka JC, Warnaar SO: Expression of intermediate-sized filaments in developing and adult human kidney and in renal cell carcinoma. J Histochem Cytochem 1990, 38:385–392
15. Störkel S, Thoenes W, Jacobi GH, Lippold R: Prognostic parameters in renal cell carcinoma: a new approach. Eur J Urol 1990, 16:416–422
16. Hoehn W, Schroeder FH: Renal cell carcinoma: two new cell lines and a serially transplantable nude mouse tumor (NC 65). Invest Urol 1978, 16:106–112
17. Matsuda M, Osafune M, Nakano E, Kotake T, Sonoda T, Watanabe S, Hada T, Okochi T, Higashino K, Yamamura Y, Abe T: Characterization of an established cell line from human renal carcinoma. Cancer Res 1979, 39:4694–4699
18. Ebert T, Bander NH, Finstad CL, Ramsawak RD, Old LJ: Establishment and characterization of human renal cancer and normal kidney cell lines. Cancer Res 1990, 50:5531–5536
19. Anglard P, Trahan E, Liu S, Latif F, Merino MJ, Lerman MC, Zbar B, Linehan WM: Molecular and cellular characterization of human renal cell carcinoma cell lines. Cancer Res 1992, 52:348–356
20. Moll R, Zimbelmann R, Goldschmidt MD, Keith M, Lauffer J, Kasper M, Koch PJ, Franke WW: The human gene encoding cytokeratin 20 and its expression during fetal development and in gastrointestinal carcinomas. Differentiation 1993, 53:75–93
21. Achtstaetter T, Hatzfeld M, Quinlan RA, Parmelee D, Franke WW: Separation of cytokeratin polypeptides by gel electrophoresis and chromatographic techniques and their identification by immunoblotting. Methods Enzymol 1986, 134:355–371
22. Moll R, Dhouailly D, Sun TT: Expression of keratin 5 as a distinctive feature of epithelial and biphasic mesotheliomas: an immunohistochemical study using monoclonal antibody AE 14. Virchows Arch B Cell Pathol 1989, 58:129–145
23. Fingert HJ, Chen Z, Mizrahi N, Gajewski WH, Bamberg MP, Kradin RL: Rapid growth of human cancer cells in a mouse model with fibrin clot subrenal capsule assay. Cancer Res 1987, 47:3824–3829
24. Vindelov L, Christensen IJ, Nissen NI: A detergent-trypsin method for the preparation of nuclei for flow cytometric DNA analysis. Cytometry 1983, 3:323–327
25. Vindelov L, Christensen IJ, Nissen NI: Standardization of high-resolution flow cytometric DNA analysis by the simultaneous use of chicken and trout red blood cells as internal reference standards. Cytometry 1983, 5:328–331
26. Seabright M: A rapid banding technique for human chromosomes. Lancet 1971, ii:971–972
27. Mitelman F (Ed): Guidelines for Cancer Cytogenetics: Supplement to an International System for Human Cytogenetics Nomenclature. Basel, S. Karger, 1991
28. Beham A, Ratschek M, Zatloukal K, Schmid C, Denk H: Distribution of cytokeratins, vimentin, and desmoplakins in normal renal tissue, renal cell carcinomas and oncocytoma as revealed by immunofluorescence microscopy. Virchows Arch A 1992, 421:209–215
29. Gerharz CD, Moll R, Störkel ST, Ramp U, Thoenes W: Ultrastructural appearance and cytoskeletal architecture of the clear, chromophilic and chromophobe cell variants of human renal cell carcinoma *in vivo* and *in vitro*. Am J Pathol 1993, 142:851–859
30. Gerharz CD, Ramp U, Olert J, Moll R, Störkel S, Marx N, Gabbert HE: Cytomorphological, cytogenetic, and molecular biological characterization of four new human renal carcinoma cell lines of the clear cell type. Virchows Arch 1994, 424:403–409
31. Franke WW, Schmid E, Schiller DL, Winter S, Jarasch ED, Moll R, Denk H, Jackson BW, Illmensee K: Differentiation-related patterns of expression of intermediate-sized filaments in tissues and cultured cells. Cold Spring Harbor Symp Quant Biol 1982, 46:431–453
32. Stetson DL, Wade JB, Giebisch G: Morphologic alterations in the rat medullary collecting duct following potassium depletion. Kidney Int 1980, 14:45–56
33. Madsen KM, Tisher CC: Response of intercalated cells of rat outer medullary collecting duct to chronic metabolic acidosis. Lab Invest 1984, 3:268–276
34. Dorup J: Ultrastructure of distal nephron cells in rat renal cortex. J Ultrastruct Res 1992, 92:101–118
35. Myers CE, Bulger RE, Tisher CC, Trump BF: Human renal ultrastructure. IV. Collecting duct of healthy individuals. Lab Invest 1966, 12:1921–1950
36. Madsen KM, Brenner BM: Structure and function of the renal tubule and interstitium. Renal Pathology. Edited by CC Tisher and BM Brenner. Philadelphia, JB Lippincott Co. 1989, pp 606–641
37. Brown D, Gluck S, Hartwig I: Structure of the novel membrane-coating material in proton-secreting epithelial cells and identification as an H^+-ATPase. J Cell Biol 1987, 105:1637–1648
38. Strange K, Willingham MC, Handler JS, Harris HW: Apical membrane endocytosis via coated pits is stimulated by removal of antidiuretic hormone from isolated, perfused rabbit cortical collecting tubule. J Membr Biol 1988, 103:17–28